A Block Matching Technique Using Unit Gradient Vectors

Toshiaki Kondo and Waree Kongprawechnon
Sirindhorn International Institute of Technology, Thammasat University
tkondo@siit.tu.ac.th, waree@siit.tu.ac.th
131 Moo 5, Tiwanont Road, Bangkadi, Muang Pathumthani 12000, THAILAND

Abstract

Irregular lighting causes temporal variations of image intensities, which makes most existing block matching techniques ineffective. For this, we propose a novel matching technique based on gradient orientation that is known to be insensitive to variations of intensities. We show that gradient orientation information can be effectively utilized by means of two intensity patterns that are obtained as the x and y components of unit gradient vectors. Simulation results show the proposed technique is remarkably robust to both spatially uniform and non-uniform changes of image intensities.

1. Introduction

Establishment of correspondence between two or more images is an important task in image sequence processing and computer vision applications. For instance, image correspondence is an essential step for estimating motions and depths. Motion estimation is concerned with the correspondence between time-sequential images such as video sequences. It finds a variety of applications, including object-based video coding (e.g. MPEG-4), object detection for surveillance systems, scene changes detection for video editing, and image stabilization technology for image acquisition devices.

Techniques for image correspondence in the spatial domain may be classified into two categories; gradient-based methods and matching methods. This paper is concerned with the latter approach that is also widely referred to as block matching, template matching, or correlation-based methods [1]-[5]. In either approach, the intensities of objects in an image are assumed to be constant over time. This assumption, however, is often violated by changes of lighting conditions that is a common incident in outdoor environment. To circumvent this irregular illumination problem, it is reasonable to employ a feature that is less dependent on image intensities or gradients.

This paper presents a novel block matching technique using gradient orientation information, rather than relying on conventional image features such as intensities and gradients, because gradient orientation is known to be insensitive to variations in illumination [6]-[9]. A comparative study with conventional block matching techniques reveals that the proposed method is remarkably robust to both uniformly and non-uniformly varying image intensities.

2. Method

2.1 Gradient orientation information

Let $I(x, y)$ be the image intensities at pixel coordinates (x, y). The gradient vectors of I may be expressed by (I_x, I_y) where I_x and I_y are the partial derivatives of I in x and y directions. Gradient orientation information (GOI) can then be expressed using unit gradient vectors (n_x, n_y) that are obtained by dividing (I_x, I_y) by their norms as

$$\left.\begin{array}{l} n_x(x, y) = I_x(x, y) \Big/ \sqrt{I_x^2(x, y) + I_y^2(x, y)} \\[2mm] n_y(x, y) = I_y(x, y) \Big/ \sqrt{I_x^2(x, y) + I_y^2(x, y)} \end{array}\right\}, \qquad (1)$$

where we assign zero to $n_x(x, y)$ and $n_y(x, y)$ when the denominator is zero to avoid zero-division.

Fig. 1(a) shows $I(x, y)$ of a test image of size 256 by 256 pixels with 256 gray levels. The upper left corner of the image is the origin, and vertical and horizontal axes are respectively denoted as x and y axes. The small region of size 32 by 32 pixels encompassed by a white square in Fig. 1(a) is cropped and enlarged in Fig. 1(b). Fig. 1(c) shows the gradient vectors (I_x, I_y) within the cropped region while Fig. 1(d) shows the unit gradient vectors (UGVs) in the same region. Note that UGVs carry rich local gradient information even in relatively low-contrast areas.
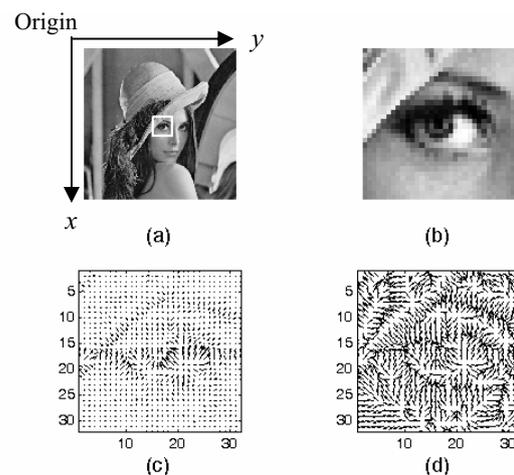
Figure 1. (a) A test image, (b) a cropped and enlarged subimage, (c) gradient vectors and (d) unit gradient vectors within the subimage.

Since UGVs are represented by two scalars n_x and n_y ranging from −1 to 1, we may easily utilize GOI by treating these scalars as intensities. Fig. 2(a) shows the gradient orientation pattern n_x corresponding to the subi-

mage in Fig. 1(b) while Fig. 2(b) shows the gradient orientation pattern n_y. Both n_x and n_y are scaled and visualized as 8-bit intensity patterns.

(a)　　　　　　(b)
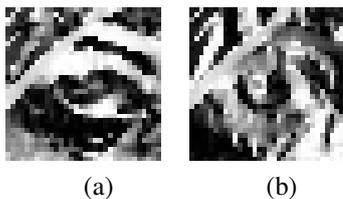
Figure 2. (a) Gradient orientation pattern n_x and (b) gradient orientation pattern n_y.

It should be stressed that the use of UGVs is computationally more efficient than using angular values θ (rad) because UGVs require no modulo calculations [9].

2.2 Intensity-invariance of gradient orientation

Gradient orientation is known to be insensitive to variations of lighting conditions [6]-[9]. This is because the order of image intensities in a local area is well preserved under varying lighting conditions. For instance, the black pupil is darker than the brown iris irrespective of illumination changes. Fig. 3 demonstrates such intensity invariance of gradient orientation. Fig. 3(a) shows the same subimage as in Fig. 1(b), except that the intensities of the upper half of it are reduced by 50%. Figs. 3(b) and 3(c) show the gradient orientation patterns n_x and n_y. The comparison between the patterns in Fig. 2 and those in Figs. 3(b) and 3(c) shows that gradient orientation patterns remain unchanged before and after shading occurs, except for slight changes along the border of the shade.

(a)　　　　　　(b)　　　　　　(c)
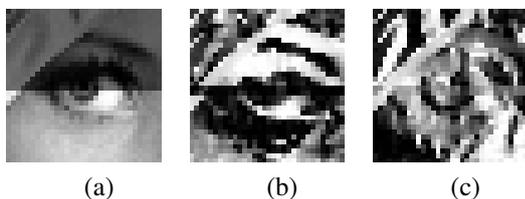
Figure 3. (a) Subimage whose upper half is shaded, (b) gradient orientation pattern n_x and (c) gradient orientation pattern n_y within the subimage.

2.3 Block matching technique with GOI

Instead of image intensities, we make use of gradient orientation patterns as inputs to a conventional block matching technique with the widely used matching metric, the sum of absolute differences (SAD) criterion:

$$
\begin{aligned}
& GOPM\_n_x(\vec{p},\vec{d}) = \\
& \sum_{j=-N/2}^{N/2}\sum_{i=-N/2}^{N/2}\left|n_{x1}(x+i,y+j)-n_{x2}(x+i+u,y+j+v)\right| \\
& GOPM\_n_y(\vec{p},\vec{d}) = \\
& \sum_{j=-N/2}^{N/2}\sum_{i=-N/2}^{N/2}\left|n_{y1}(x+i,y+j)-n_{y2}(x+i+u,y+j+v)\right|
\end{aligned} \tag{2}
$$

where $\vec{p}$ denotes a point (x,y) in the image coordinate,

$\vec{d}$ a displacement (u,v) from that point, equivalent to the motion vector between two time-sequential images being compared, N the block size, n_{x1} and n_{y1} gradient orientation patterns of the first frame (reference image), and n_{x2} and n_{y2} the second frame where a best-matching block is being searching for. Finally, these two may be combined into one measure

$$
\begin{aligned}
& GOPM(\vec{p},\vec{d}) = \\
& GOPM\_n_x(\vec{p},\vec{d}) + GOPM\_n_y(\vec{p},\vec{d})
\end{aligned} \tag{3}
$$

The position of the best matching is indicated by the minimum of Eq. (3). We call this proposed method the gradient orientation pattern matching technique (GOPM). Note that we also have evaluated the sum of squared differences (SSD) criterion, but there was no noticeable improvement of performance.

3. Results and Discussion

3.1 Simulations on synthetic image sequences

We compare GOPM with SAD block matching (SAD) and zero-mean normalized cross-correlation (ZNCC) on four synthetic image sequences. Four standard test images of size 256 by 256 pixels with 256 gray levels are used as the first frames or references. The second frames are then generated by translating them by 5 pixels both horizontally and vertically. We have computed 225 (15 by 15) motion vectors in each sequence. The size of the block is fixed at 16 by 16 pixels. The range for searching for the best matching position in the second image is set at ± 8 pixels both horizontally and vertically. When a motion vector points a correct pixel, it is considered as a successful motion estimate. To make the simulation realistic, zero-mean Gaussian noise is randomly generated and added to every image where the SNR is set at approximately 40dB. Further, to test the robustness to varying lightings, the intensities of the second image are modified in four ways. One is a uniform reduction of intensities, and the other three are non-uniform modifications of intensities achieved by multiplying the masks shown in Fig. 4. Figs. 4(a) and 4(b) show realistic smooth linear and Gaussian shadings. Fig. 4(c), on the other hand, shows rapidly varying shadows that may simulate the case that a spot light is flashed on an object.

(a)　　　　　(b)　　　　　(c)
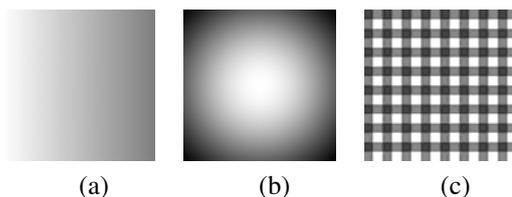
Figure 4. (a) Linear shadow mask, (b) Gaussian shadow mask and (c) checkerboard shadow mask.

Table 1 shows the successful motion estimation rates (%) by the three methods in which the second images are subject to the uniform intensity reduction by 20% (Simu-

lation 1). It is evident that SAD does not work at all while ZNCC and GOPM work nearly perfectly. Tables 2 and 3 show the success rates under non-uniform but smooth changes of image intensities. In Simulation 2, linear shading is applied to the second images where intensities are linearly reduced from the left to the right end of the image up to 50% (Fig. 4(a), Table 2). In Simulation 3, Gaussian shading is applied so that intensities are reduced from the center of the image following the profile of a Gaussian function (Fig. 4(b), Table 3). Under non-uniform but smooth variations of intensities, both ZNCC and GOPM achieve high success rates. Unsuccessful motion estimates are due to the lack of gradient information (e.g. sky) and the aperture problem.

In Simulation 4, rapid and non-uniform shading is applied in which the image intensities in vertical and horizontal stripes are reduced to 50% and the intensities in the areas where two stripes overlap are reduced to 25% (Fig. 4(c)). ZNCC can cope with both additive and multiplicative variations of intensities when those variations occur uniformly within a block. By contrast, GOPM can handle such rapid and non-uniform intensity changes within a block, which is highlighted in Table 4.

Table 1. Success rates under a mildly noisy condition with uniformly varying image intensities.

Simulation 1	SAD	ZNCC	GOPM
Lena	24.9	100	100
Girl	27.1	100	100
Cameraman	40.9	97.8	98.2
House	4.90	99.6	96.4

Table 2. Success rates under a mildly noisy condition with linear shading.

Simulation 2	SAD	ZNCC	GOPM
Lena	25.8	99.1	100
Girl	27.1	100	100
Cameraman	39.1	98.7	99.1
House	4.89	97.3	96.0

Table 3. Success rates under a mildly noisy condition with Gaussian shading.

Simulation 3	SAD	ZNCC	GOPM
Lena	44.9	97.3	99.6
Girl	21.3	100	99.6
Cameraman	36.9	98.2	97.3
House	41.8	94.2	92.9

Table 4. Success rates under a mildly noisy condition with rapid and non-uniform shading.

Simulation 4	SAD	ZNCC	GOPM
Lena	10.2	20.0	97.3
Girl	13.8	26.2	100
Cameraman	13.3	33.3	91.6
House	2.2	5.33	88.0

3.2 Simulations on real image sequences

We next evaluate the performances of SAD, ZNCC, and GOPM on two real image sequences, A and B. Since there is no ground truth data (i.e., true motion vectors) available for these real sequences, we use the motion vectors estimated under a constant illumination as references shown in the left column of Fig. 5. Fig. 5 shows the image sequence A in which the camera tracks a walking man. The motion vectors in background are supposed to point rightward while those on the man are small. Under such ideal lighting condition, the motion estimates by the three methods are similar to each other. We then apply the same four intensity modifications as in 3.1. The robustness of motion estimation is evaluated in terms of the means and variances (m, σ^2) of the differences between the references and the motion vectors estimated under varying lighting conditions. Table 5 shows the differences when the second image is subject to a uniform change of intensities as described in Simulation 1. SAD shows large variances while those of ZNCC and GOPM are far smaller, indicating that the latter two methods work robustly with uniform variations of intensities. Tables 6 and 7 show the differences when the second image is subject to non-uniform but smooth changes of intensities as depicted in Simulations 2 and 3. SAD fails to estimate motion reliably. Conversely, ZNCC and GOPM withstand such lighting conditions. Finally, Table 8 shows the differences when the second image is subject to rapid and non-uniform changes of intensities as in Simulation 4. As shown in the right column of Fig. 5, SAD and ZNCC fail to work properly under such condition, while GOPM still estimates reasonably accurate motion vectors.

Table 5. Differences in the estimated motion vectors before and after uniform shading is applied.

Sim 1	SAD	ZNCC	GOPM
Image A	(5.02, 24.0)	(0.016, 0.02)	(0.067, 0.25)
Image B	(3.51, 21.5)	(0.067, 0.55)	(0.19, 1.77)

Table 6. Differences in the estimated motion vectors before and after linear shading is applied.

Sim 2	SAD	ZNCC	GOPM
Image A	(6.19, 31.1)	(0.013, 0.63)	(0.11, 0.41)
Image B	(3.67, 20.3)	(0.36, 3.46)	(0.34, 2.79)

Table 7. Differences in estimated motion vectors before and after Gaussian shading is applied.

Sim 3	SAD	ZNCC	GOPM
Image A	(5.77, 22.5)	(0.78, 4.74)	(0.22, 0.84)
Image B	(4.19, 28.1)	(0.98, 9.62)	(0.70, 5.44)

Table 8. Differences in estimated motion vectors before and after rapid and non-uniform shading is applied.

Sim 4	SAD	ZNCC	GOPM
Image A	(6.99, 17.9)	(5.93, 24.7)	(0.88, 4.11)
Image B	(5.21, 20.5)	(3.69, 23.5)	(0.77, 5.30)
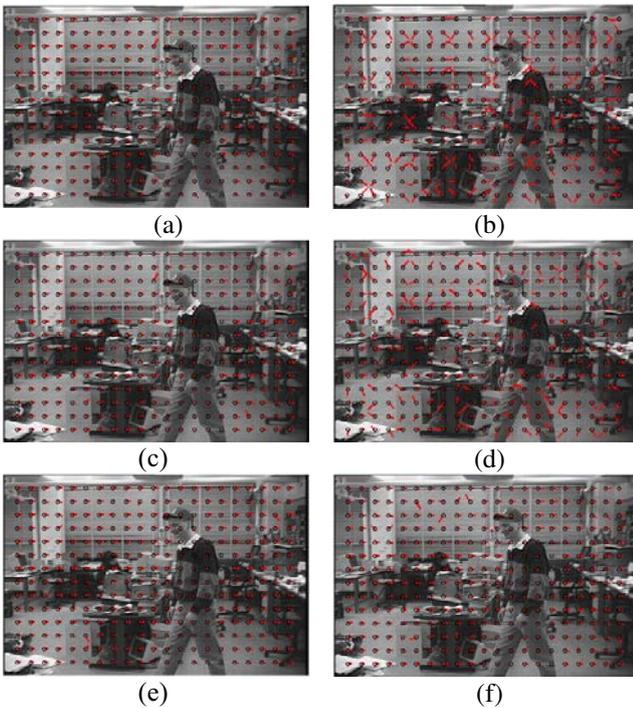
Figure 5. Motion vectors estimated by (a), (b) SAD, (c), (d) ZNCC and (e), (f) GOPM under constant (left column) and varying lighting conditions (right column).

3.3 Computational cost

We have compared the computational costs of SAD, ZNCC, and GOPM. Table 9 shows the computation time of each method for computing 225 motion vectors. The three techniques are implemented in MATLAB (Ver. 7.0) and executed on a PC with the Pentium 4 (2.80GHz) and 1GB of RAM. SAD is the fastest method among the three owing to its simplest similarity measure whereas ZNCC is the slowest because of the complexity of its computation [4]. GOPM is slower than SAD because GOPM requires an extra computation of Eq. (1) and also two sums-of-differences have to be computed as in Eq. (2). It is important to note that GOPM is faster than ZNCC. GOPM can be computed more efficiently than ZNCC because the similarity measure of GOPM is the same as that of SAD which is much simpler than that of ZNCC. Another advantage of GOPM is that it allows the use of integers while real numbers are necessary for ZNCC.

Table 9: Computation times of SAD, ZNCC, and GOPM.

	SAD	ZNCC	GOPM
Computation time (sec)	0.94	3.97	1.47

4.   Conclusions

Most existing approaches for image matching are based on either image intensities or gradients. Consequently, it is inevitable that these conventional techniques are susceptible to varying image intensities caused by irregular lighting conditions. To cope with this illumination prob-lem, we have presented a novel matching technique that is based on gradient orientation patterns that can be obtained as the x and y components of unit gradient vectors. We do not use the angular values θ (rad) of gradient vectors directly to avoid modulo computation, which enables a fast implementation of the proposed method. Simulation results on both synthetic and real image sequences have revealed that the proposed technique, GOPM, works much more robustly than SAD with varying image intensities. The motion estimation performance of GOPM is comparable to that of ZNCC with uniformly changing intensities and also non-uniformly but smoothly varying intensities. Furthermore, it is a significant advantage of GOPM over ZNCC that it can cope with non-uniform and rapid changes of image intensities that may occur in outdoor environment. We have also shown that the computational cost of GOPM is less than that of ZNCC. Gradient vectors are generally computed at an early stage of various image processing and computer vision applications, and are readily available. The normalization of the gradient vectors to obtain the unit gradient vectors can be performed prior to the computation for image correspondence. Therefore, GOPM will be well-suited to real-time applications and also hardware implementation.

References

[1] T.R. Reed, *Digital Image Sequence Processing, Compression, and Analysis*, CRC Press, 2005.

[2] R. Jain, R. Kasturi, and B.G. Schunck, *Machine Vision*, McGraw-Hill, Inc., 1995.

[3] R.C. Gonzalez and R.E. Woods, *Digital Image Processing*, Prentice-Hall, Inc., 2008.

[4] A. Giachetti, "Matching techniques to compute image motion," *Image and Vision Computing*, 18, pp. 247-260, 2000.

[5] M. Ye, R.M. Haralick, and L.G. Shapiro LG, "Estimating piecewise-smooth optical flow with global matching and graduated optimization," *IEEE Trans. Pattern Anal. Machine Intell.*, Vol. 25, No. 12, pp. 1625-1630, 2003.

[6] P.H. Gregson, "Using angular dispersion of gradient direction for detecting edge ribbons," *IEEE Trans. Pattern Anal. Machine Intell.*, Vol. 15, No. 7, pp. 682-696, 1993.

[7] T. Kondo and H. Yan, "Automatic human face detection and recognition under non-uniform illumination," *Pattern Recognition*, 32, pp. 1707-1718, 1999.

[8] H.F. Chen, P.N. Belhumeur, and D.E. Jacobs, "In search of illumination invariants," *Proceedings of the IEEE Int'l Conf. on Comp. Vision and Pattern Recognition*, 1, pp. 254-261, 2000.

[9] P.Y. Burgi, "Motion estimation based on the direction of intensity gradient," *Image and Vision Computing,* 22, pp. 637-653, 2004.